When do Rocks Move? Sediment Transport and Geomorphic Processes in the Italian Alps, Switzerland

by Elizabeth Wong
May 5th 2008
Research and Senior Thesis for the Geology & Geophysics major
Adviser: Mark Brandon, Alison Anders

1. Introduction

Rivers are the primary control of erosion in the absence of significant glacial processes, and they do so by incising into bedrock and transporting the sediment out of the system. Previous studies on erosion use stream power law to characterize incision, in which the bedrock incision rate, E, is a function of river slope, *S*, and discharge, *Q*: $E = k Q^m S^n$, where k, m and n are controls on discharge and slope (see Whipple, 2002). However, rivers can only incise if the bedrock is exposed in the first place (Howard and Kerby, 1983) – implying that erosion rates are dependent on bedload transport. Most bedrock rivers have a thin seasonal alluvial cover, so floods have to be large enough to be able to transport the alluvial cover before incision can occur. Hence, more realistic models incorporate a minimum threshold (either a unit critical discharge or a critical shear stress term) where no sediment transport occurs until this threshold is reached. Mueller and Pitlick (2005) propose a bedload transport model that is a function of excess shear stress – that is, shear stress greater than the amount needed to carry the sediment.

In turn, the amount of sediment transport is dependent on the frequency and magnitude of flood events. Wolman and Miller (1960) show that for alluvial rivers, frequent small floods with recurrence interval of one to two years are the most geomorphically-effective floods – that is, flood events that transport the largest fraction of the annual sediment yield. Rare (defined here as having a recurrence interval greater than 50 years) large floods carry only a small fraction of the annual sediment yield, as these floods are so infrequent.

In this study, we look at rivers in the Lepontine Dome in the southern Alps. This region experiences more precipitation than the surrounding regions, greater on the order of two to five times (Frei and Schar, 1998). This high precipitation intensity coupled with rapid erosion rates may affect tectonic uplift rates of the region. (Anders et al. 2002). The purpose of this study is to

examine how precipitation intensity and flood events are linked to sediment transport in this region, and what these relationships imply about erosion rates and tectonic uplift.

2. Study Area

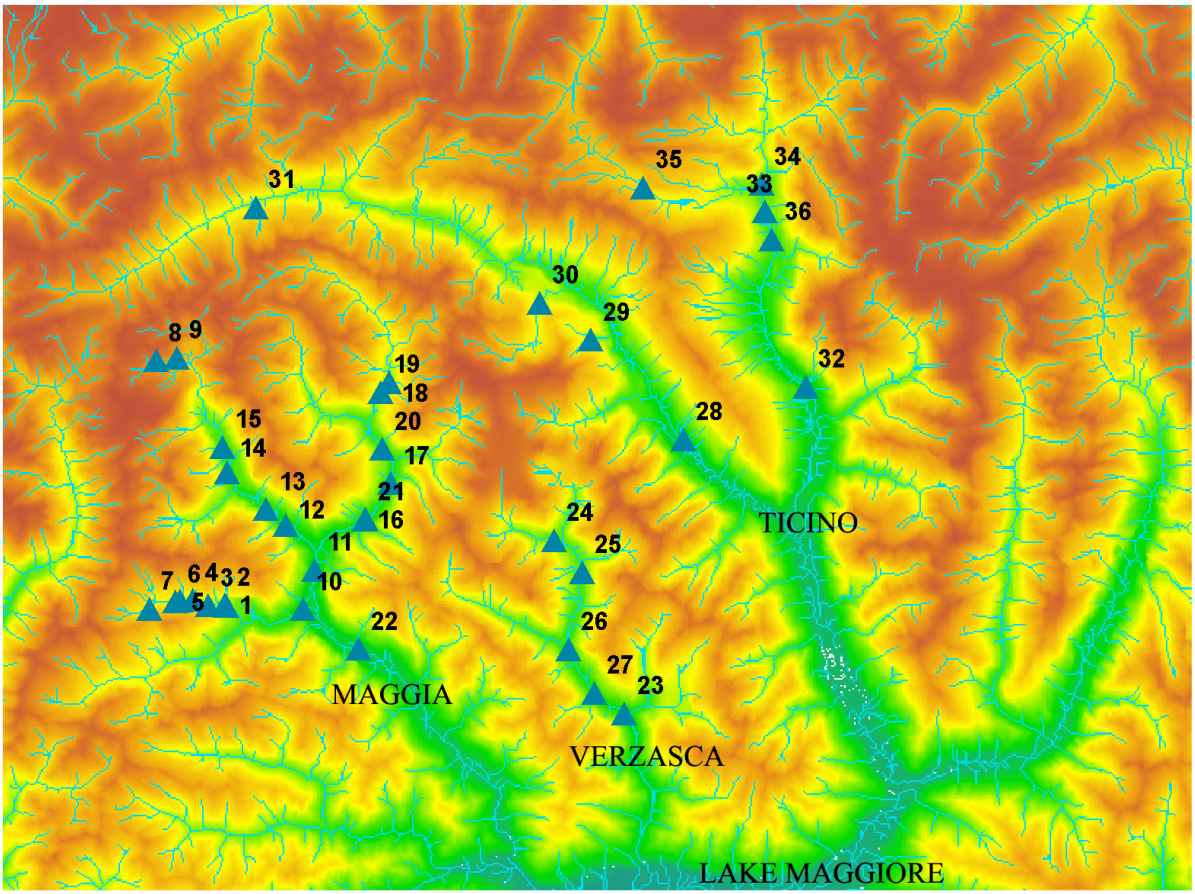

Figure 1. Topographic map of the Ticino canton, Switzerland, showing study sites numbered 1 to 36 along three major rivers (Maggia, Verzasca and Ticino) and their tributaries. All three rivers drain into Lake Maggiore.

Figure 1: Topographic map of the Ticino canton, Switzerland, which shows the location of study sites numbered 1 to 36. The study sites are located along three major rivers – Maggia, Verzasca and Ticino – and their tributaries. All three rivers drain into Lake Maggiore.

The Lepontine Dome is located in the Lago Maggiore region of the Ticino canton. There are three major rivers in the region: the Maggia, Verzasca and Ticino rivers, all originating from the southern rim of the Alpine ridge and drains into Lago Maggiore. The location of these rivers

and Lago Maggiore, along with the study sites from 1 to 36, are labeled on Figure 1, which is a topographic map of the Lago Maggiore region. The cumulative drainage area encompassed by all three rivers is approximately 700 km^2. The elevation of the region ranges from 200 to 3000 meters.

Evidence of Quaternary glaciation is demonstrated in the basin morphology. The region is characterized by rivers incising into both Quaternary moraine deposits in broad U-shaped valleys (with evidence of floodplain features), and bedrock channels that form narrow gorges. These rivers are generally overlain with a thin discontinuous alluvial cover. Local relief is greatest in rivers that are deeply incised into bedrock. The entire area is underlain by highly metamorphosed and very resistant bedrock, the product of orogenic collision between the Adriatic and European plates.

The annual precipitation of this region ranges from about 2 to 6 mm day^{-1}. Precipitation reaches a maximum in May and a secondary maximum in October. Winter months are generally drier than summer months. The Ticino canton is known to be affected by flash-flooding especially during the summer months, because of the extreme precipitation events coupled with local conditions – rivers with narrow channel widths and are confined by bedrock, frequent floods which leads to shorter recovery times and thin soil covers (Frei and Schar, 1998).

3. Methods

3.1 Measurements

Trends in erosion rates and sediment transport capacities were estimated by calculating the annual sediment yield. Estimates of these rates are made through measuring the following

channel characteristics at 36 sites along the three rivers – Maggia, Verzasca, Ticino – and their tributaries:

a) local channel slope, S
b) channel width at bankfull condition, W
c) grain sizes of the coarse surface layer

Each study site was selected based on its accessibility and the absence of other factors that might complicate calculations, like braiding or modification of channel morphology due to anthropogenic influence (construction of artificial structures like small dams and bridges, or presence of farms that might add to the sediment input). Figure 2 shows an example of a characteristic study site.

Figure 2: A characteristic example of study reach. This is the view upstream of study site 20 on the River Maggia. Slope, width and grain sizes were measured at each site whenever possible.

3.2 Calculations

3.2.1 Critical shear stress, τ_c (the minimum shear stress needed for entrainment of a grain with a diameter of size *D*).

Several studies have proposed empirical relationships that links grain size directly to critical shear stress, stream power or discharge (e.g. Baker and Ritter, 1977; Costa 1983; Williams, 1983). However, these empirical relations do not account for the selective entrainment effect that occurs in deposits of mixed sizes. In a deposit of mixed grain sizes, such as the bed material (the coarse surface layer) of rivers, entrainment is a function of grain size relative to the the ambient size population (Komar, 1987; Ferguson, 1994). Hence, a more realistic model is one that incorporates the effect of the ambient size population. Komar (1987) proposes an expression derived from the classic Shields criterion equation that accounts for selective entrainment. This formulation estimates the critical shear stress τ_c needed to entrain a particular grain size *D* relative to the reference grain size of the bed material, D_{84}:

$$\tau_c = 0.045(\rho_s - \rho)gD_{84}^{\ 0.6}D^{0.4} \qquad (1)$$

where ρ_s is the density of the clasts (2650 kg/m^3), ρ is the density of water (1000 g/m^3) and *g* is gravitational acceleration. We substitute *D* with D_{84} to obtain estimates of $\tau_{c\,(D84)}$, listed in a column in Table 1. This equation as proposed by Komar (1987) will be used for all calculations of τ_c in this paper, as it has the advantage of being dimensionally-correct and theoretically-based.

We should also point out that Komar (1987) uses the median grain size of the bed material, D_{50} as the reference grain size. Lenzi et al. (2006), working in a steep boulder-bed channel in the Italian Alps, suggest that a larger grain size like D_{84} or D_{90} might be more appropriate as the reference diameter for boulder-bed channels, as these grain sizes are able to characterize bed roughness and bed forms (which in turn characterize flow resistance) with more

accuracy. Moreover, the channel morphologies of the rivers in the Lepontine Dome – mostly steep, shallow mountain rivers with rough beds – are comparable to the ones in Lenzi et al.(2006)'s study. Therefore, the substitution of D_{84} for the oft-used D_{50} as the reference diameter to characterize the bed material appears reasonable. Henceforth, all calculations in this paper will use D_{84} in place of D_{50} as the reference grain size.

3.2.2 Critical unit discharge, q_c (minimum discharge per unit width needed for entrainment of a grain with a diameter of size D).

Komar (1987)'s estimate of critical shear stress τ_c can be converted into critical unit discharges. The use of critical discharge might be preferable to shear stress, as shear stress estimates not only require the knowledge of gross-channel properties like width and depth, but also within-channel conditions like flow depth, which is locally variable (Jansen, 2006; Ferguson, 1994). While shear stress may be locally variable, discharge remains constant despite local changes in channel width and slope.

Several steps have to be taken to convert from shear stress to discharge. Consider that at the point of entrainment, boundary shear stress is equal to or greater than critical shear stress. Therefore, boundary shear stress can be equated critical shear stress to obtain minimum flow depth d_c that would entrain a grain of size D:

$$\tau_c = \tau = \rho g d_c S \qquad (2)$$

Using minimum flow depth, d_c, cross-section average velocity U can be calculated using the empirical Manning (1981) equation, where hydraulic radius R is substituted for d_c:

$$U = \frac{d_c^{2/3} S^{1/2}}{n} \qquad (3)$$

Finally, critical unit discharge q_c can be estimated through the equation:

$$q_c = \frac{\tau_c U}{W_{bf}} \quad (4)$$

Ferguson (1994) formulates a different expression for critical unit discharge, using a modified version of Shields' criterion (accounting too for relative size) and the Darcy-Weisbach empirical flow resistance law:

$$q_c = \frac{aD_{84}}{S^{c+1}}\left(\frac{D}{D_{84}}\right)^{(1-x)(c+1.5)} \quad (5)$$

$$\text{where } a = m(8g)^{0.5}\left(\left(\frac{\rho_s}{\rho}-1\right)\tau_{c*84}\right)^{c+1.5} \quad (6)$$

where x is the hiding factor (x=0.90; Parker, 1990), m and c are constants found in the flow law (c=0.37, m=1.14; Thompson and Campbell, 1979), and τ_{c*84} is the critical dimensionless shear stress (τ_{c*84} = 0.045). Ferguson's (1994) q_c estimates can also be found in Table 1.

Figure 3 compares q_c estimates derived from Komar (1987)'s formulation of τ_c, and from Ferguson (1994)'s formulation. The plot shows a nearly perfect one-to-one correlation between both estimates. This correlation is despite the fact that both derivations have different theoretical basis. The excellent correlation attests to the validity of either methods, suggesting that the estimates are interchangeable and can be used in place of the other estimate whenever the calculations should require this. Therefore neither shear stress nor discharge is a superior estimate to the other, as they are exchangeable for each other (Ferguson, 2005; Lenzi et al., 2006).

In this paper, both critical shear stress and critical discharge will be used in estimating the frequency and magnitude of the discharge that transports sediment, and total sediment transport capacity for the system.

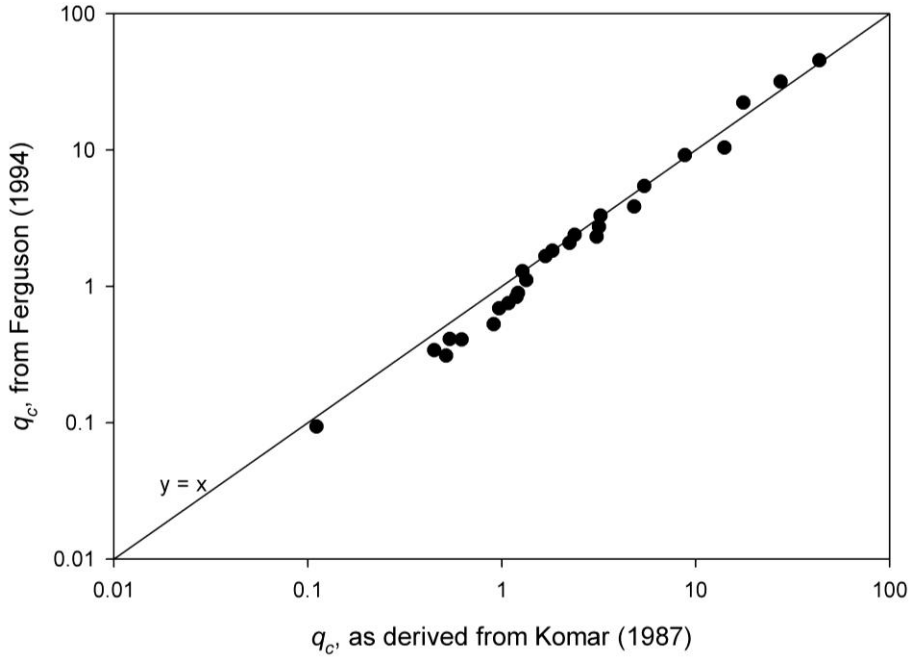

Figure 3 shows critical unit discharge q_c, estimated by two different studies, Komar (1987who derived an expression for critical shear stress, and Ferguson (1994) who used the Darcy-Weisbach flow-resistance law. Note the excellent one-to-one agreement between the two estimates, despite their differing theoretical basis.

3.2.3 Bedload transport capacity, Q_s

The bedload transport capacity Q_s represents the instantaneous maximum amount of bed material that can be transported out of the system (assuming that the system is transport-limited). Mueller and Pitlick (2005) employs the concept of equal mobility in formulating an expression for bedload transport capacity Q_s, where the amount of bed material transported is a function of excess shear stress, $(\tau^* - \tau^*_c)$.

$$Q_s = 11.2\left((s-1)gD_{84}{}^3\right)^{0.5} \frac{\left(\tau^* - \tau^*_c\right)^{4.5}}{\tau^{*3}} W_{bf} \qquad (7)$$

$$\text{and } \tau^* = \frac{\tau}{(\rho_s - \rho)gD_{84}} \qquad (8)$$

where τ^* is the dimensionless boundary shear stress, τ^*_c is the dimensionless reference shear stress (as referred to earlier, τ^*_c =0.045), s is the specific gravity of sediment (s=2.65). The value for mean boundary shear stress τ is averaged across the channel and depends on the depth-slope product:

$$\tau = \rho g d S \qquad (9)$$

Since we do not have local measurements of bankfull depth at the study sites, we have to make an estimate for bankfull flow depth. Finnegan et al. (2005) observes that the ratio of width-to-depth in natural channels (α) is constant, and its value depends on the channel substrate (e.g. bedrock, boulder, cobble, gravel). However, the claim of a constant width-to-depth ratio for a particular channel substrate has not been given a rigorous scientific treatment by the authors. In fact, Whittaker et al. (2007) shows that for three rivers in Central Apennines, Italy, which are in transient state and have not reached a topographic equilibrium, the width-to-depth ratio varies strongly with channel slope. However, for the purposes of estimating τ (and because there is no other way of estimating flow depth at bankfull condition), we assume that there is a constant width-to-depth ratio. With width measurements and knowledge of the channel substrate, bankfull flow depth d can be estimated in the following relation:

$$d = \frac{W}{\alpha} \qquad (10)$$

Substituting equation (10) into (9), we get an equation that predicts mean boundary shear stress τ at bankfull:

$$\tau = \frac{\rho g W S}{\alpha} \qquad (11)$$

The mean boundary shear stress τ is transformed into a dimensionless number τ^* using Equation 8, and these values are listed in a column in Table 1.

Lastly, our estimates of dimensionless mean boundary shear stress τ^* and critical shear stress τ^*_c, along with measurements of channel dimensions like width and grain size distribution, allows us to use Equation (8) to calculate the bedload transport capacity Q_s for all of our 36 study sites. Our estimates of Q_s are listed in Table 1.

3.2.4 Total sediment transport capacity, Q_t

Total sediment yield (normalized to the upstream drainage area) Q_t is estimated:

$$Q_t = \frac{Q_s}{\alpha A} \qquad (12)$$

where A is the upstream drainage area in m^2, and α is the fraction of bedload material in total sediment carried by the river. In mountain streams, the fraction of bedload to total amount of sediment is about 0.1 to 0.8 (for references, see p. 120-121, Wohl, 2000). For purposes of this calculation a mid-value of 0.3 is used.

3.2.5 Cumulative probability distribution of daily mean discharge.

Three of our study sites, site 11, 28 and 32, lie within 100 meters upstream or downstream of gauging stations – Maggia-Bignasco, Ticino-Pollegio and Brenno-Loderio stations. These study sites each lie on one of the three major rivers, Maggia, Ticino and Brenno, allowing comparisons between different rivers. Each of the gauging stations has at least 15 years of discharge records (1993-present). This data was obtained from the website of The Federal Office for the Environment (FOEN).

The discharge data from the gauging stations were weighted with upstream drainage area A. This correction accounts for the differences in discharge between the gauging station and the associated study site due to the drainage area alone. The assumption behind this correction is

that, for the points along a river, the variability in upstream drainage area *A* controls the overall variability in discharge – ignoring other factors such precipitation. However, since the study sites are close to the associated gauging station, only within 100 meters of each other, this assumption is a reasonable one.

We calculate the cumulative probability distribution $P(\geq Q)$ of fifteen years of daily mean discharges (1/1/1993-12/31/2007) for all three study sites, where $P(\geq Q)$ is the fraction of time during which the daily mean discharge is equaled to are exceeded. In Figure 4, we plot cumulative probability $P(\geq Q)$ against daily mean discharge *Q*. There are 5480 data points in this distribution, with each data point representing the daily mean discharge for each day during the total interval considered.

The cumulative probability distribution are fit to a power-law distribution in Figure 4, as Malamud and Turcotte (2006) show good power-law behaviour in the cumulative probability distribution of daily mean discharges. The discharge data was trimmed below a particular cut-off point, when the curve deviated significantly from a power-law fit (when $P(\geq Q)$ is very small). The power-law distribution can be described as:

$$P(\geq Q) = CQ^{-\beta} \qquad (13)$$

where *C* and β are constants.

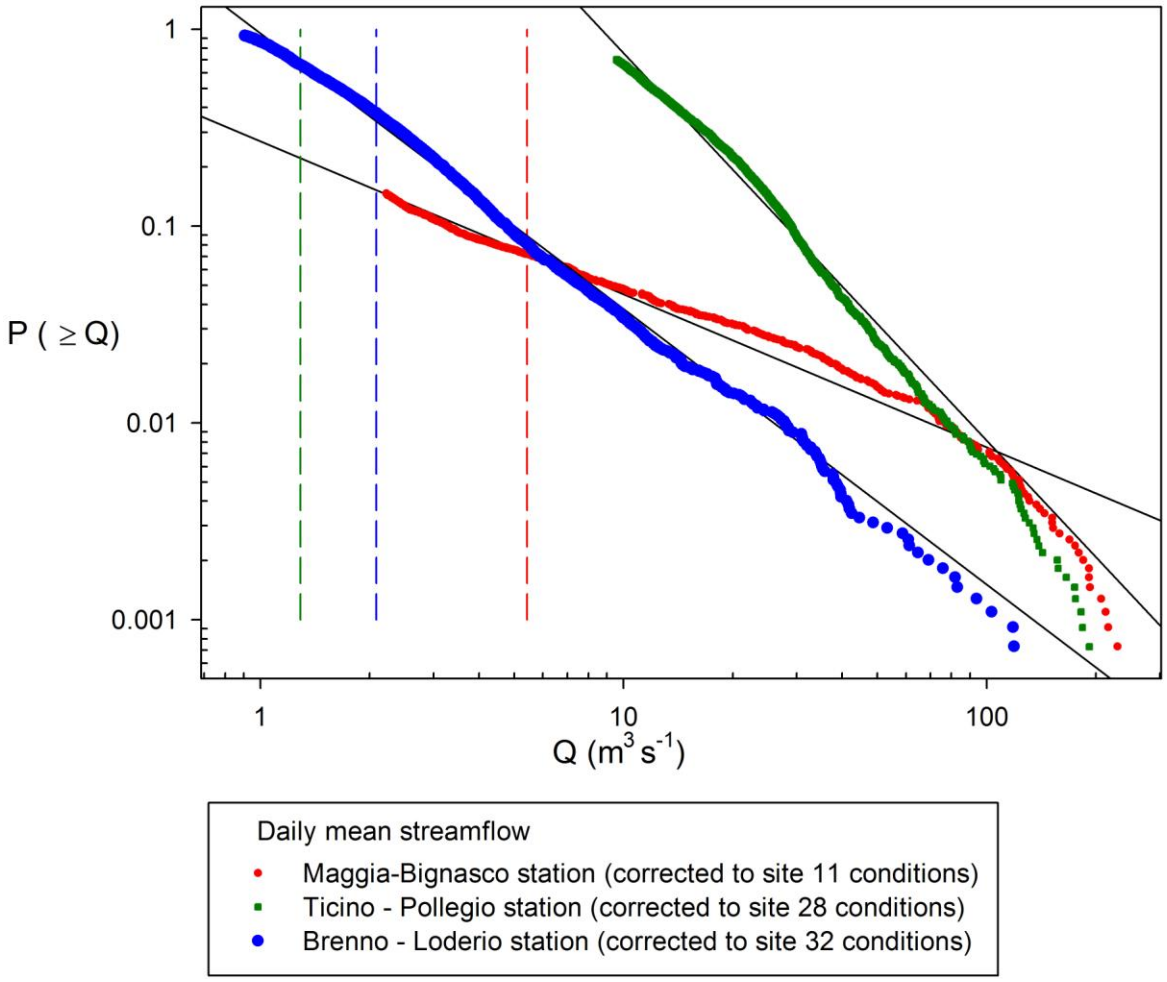

Figure 4 is a plot of cumulative probability *P(≥Q)* against daily mean discharge *Q* for three gauging stations (data obtained from FOEN): Maggia-Bignasco, Ticino-Pollegio and Brenno-Loderio. These three gauging stations correspond to a particular study site within 100m upstream or downstream: study site 11, 28 and 32 respectively. The cumulative probability is the fraction of time during which the daily mean discharge is equaled to or exceeded in the total interval considered. The cumulative probability distributions for all three sites are fitted to a power-law distribution, shown by the solid straight lines. The dashed vertical lines represent the critical discharges Q_c to entrain $D_{84.}$ All discharge values to the right of the dashed line (discharges greater than the critical discharge) will start to move bed material.

3.2.6 Total sediment transport capacity $\dot{Q}_t$, weighted by frequency.

Using the power-law fit of cumulative probability distribution of discharge (Equation 13) and the expression for bedload transport capacity Q_s (Equation 7), we calculate frequency-

magnitude distribution for discharge *Q*. For the three study sites where we have discharge records, we use this frequency-magnitude distribution to predict a mean bedload transport capacity $\overline{Q_s}$, and using Equation 12 to get a total sediment transport capacity $\dot{Q}_t$. Here are the steps of our calculation:

1) We calculate *Q* for each increment of the recurrence interval of floods, *T*. Given that the power-law fit of the cumulative probability distribution of daily mean discharges is linked to the power-law fit of the partial-duration flood series (Malamud and Turcotte, 2006), *Q* can be written as a function of *T*, where:

$$Q(T) = (CT)^{1/\beta} \qquad (14)$$

Increments of T = 1 day were small and accurate enough for this step-wise integration. We perform this step-wise integration of *Q(T)* from T: 1 to 37960 days. (This upper-limit of *T* = 37960 days was obtained by Werner (2008), who used lichenometry to date biggest boulders that were moved in the largest flood events in the region.) We assume that the age of the boulders represents the highest-magnitude flood which is possible given a particular set of climatic conditions.

2) We back-calculate the boundary shear stress τ from *Q (T)* for each increment of *T* (*T*: 1 to 37960 days), using Equation 4, 3 and 2.

3) τ (for each *Q(T))* and τ_c are converted into dimensionless numbers τ^* and τ^*_c using Equation 8. Then we calculate the bedload transport capacity $Q_s = f((\tau^* - \tau^*_c), T)$ for each increment of *Q(T)* and *T* (*T*: 1 to 37960 days).

4) We calculate $dP(\leq Q)/dQ$ for each increment of *T*, where $\frac{dP(\leq Q)}{dQ} = -C\beta Q^{\beta-1}$

5) We multiply $dP(\leq Q)/dQ$ and *Q(T)* for each increment of *T* to get the mean bedload transport capacity $\overline{Q_s}$, in units of cubic meters per year:

$$\overline{Q_s} = \sum_{j=1}^{37960} Q_s(j) \frac{dP(\leq Q)}{dQ}(j)$$

6) Finally, we calculate the total sediment transport capacity $\dot{Q}_t$, in units of meters per year using Equation (12):

$$\dot{Q}_t = \frac{\overline{Q_s}}{\alpha A}$$

where *A* is the upstream area of the drainage in m^2 and α is the fraction of the bedload relative to the total sediment load. As addressed above, the value of α is taken to be 0.3.

Table 1: Study Site Characteristics

Study site	Nearest Gauging Station	D_{50} (m)	D_{84} (m)	S (m/m)	W_{bf} (m)	A (km^2)	$\tau_{c\,(D84)}$ (N/m^2)	$Q_{c\,(D84)}$ (m^3/s)	τ^*	Q_s (m^3/km^2/yr)	Q_t (m/yr)
1		0.064	0.128	0.088	8.3	26.1	93.2	0.83	0.69	3100000	10.386
2		0.032	0.127	0.073	7.0	22.9	92.1	0.89	0.48	540000	1.796
3		0.045	0.091	0.081	5.1	21.1	65.9	0.34	0.56	950000	3.155
4		0.045	0.128	0.091	7.9	18.8	93.2	0.75	0.68	2400000	8.020
5		0.064	0.128	0.122	6.3	15.7	93.2	0.41	0.73	4400000	14.500
6		0.045	0.091	0.078	5.9	14.1	65.9	0.41	0.62	2000000	6.606
7		0.064	0.128	0.047	16.1	6.2	93.2	3.83	0.39	8500000	28.412
8		0.045	0.091	0.023	--	1.4	65.9	--	--	--	--
10		0.045	0.128	0.036	8.0	101.0	93.2	2.73	0.27	70000	0.234
11	Maggia-Bignasco	0.032	0.064	0.026	28.2	300.2	46.6	5.43	0.76	380000	1.274
12		0.045	0.091	0.008	14.8	102.1	65.9	22.18	0.09	2700	0.009
13		0.032	0.091	0.010	28.9	93.9	65.9	31.62	0.23	99000	0.330
14		0.064	0.091	0.025	5.6	62.0	65.9	1.82	0.10	5600	0.019
15		0.032	0.045	0.082	4.0	1.0	33.0	0.09	0.21	1100000	3.625
16		0.032	0.064	0.064	20.1	159.7	46.6	1.11	2.42	3600000	11.856
17		0.045	0.091	0.042	--	152.6	65.9	--	--	--	--
18		0.045	0.091	0.018	17.0	58.1	65.9	9.13	0.40	590000	1.975
19		0.032	0.064	0.027	13.1	59.5	46.6	2.38	0.66	700000	2.349
20		0.064	0.257	0.043	13.5	113.3	187.5	10.39	0.27	170000	0.564
21		0.032	0.064	0.064	20.1	159.6	46.6	1.11	2.42	3600000	11.864
22		0.032	0.091	0.006	--	436.3	65.9	--	--	--	--
23		0.032	0.045	0.020	--	125.6	33.0	--	--	--	--
24		0.045	0.064	0.029	10.1	20.8	46.6	1.66	0.31	550000	1.837
25		0.032	0.064	0.024	15.9	55.8	46.6	3.29	0.40	350000	1.169
26		0.045	0.128	0.013	32.7	103.5	93.2	45.32	0.40	640000	2.126
27		0.064	0.128	0.030	--	112.8	93.2	--	--	--	--
28	Ticino-Pollegio	0.023	0.045	0.033	15.7	341.3	33.0	1.29	0.33	21000	0.070
29		0.045	0.128	0.183	8.4	5.3	93.2	0.31	1.46	33000000	109.631
30		0.032	0.091	0.101	14.1	18.6	65.9	0.69	1.91	15000000	48.534
31		0.064	0.128	0.206	16.9	3.4	93.2	0.53	3.30	650000000	2182.00
32	Brenno-Loderio	0.032	0.064	0.036	17.6	245.3	46.6	2.08	0.68	240000	0.792
34		0.045	0.128	0.037	--	100.5	93.2	--	--	--	--
35		0.011	0.023	0.007	--	22.6	16.5	--	--	--	--
36		0.064	0.133	0.061	13.1	163.3	96.9	2.31	0.72	850000	2.845

Nearest Gauging Station: A particular study site has 15 years of discharge records, if there is a gauging station on the same river and 100m upstream or downstream from the study site. D_{50} and D_{84} refers to the median and 84th percentile grain size of the course surface layer, respectively. S is the slope, W_{bf} is the bankfull width of the channel. At several sites, width measurements are unavailable, which in turn affected estimates of Q_c. A indicates the upstream drainage area. $\tau_{c\,(D84)}$ is the critical shear stress needed to move the D_{84}, as estimated from Komar (1984). $Q_{c\,(D84)}$ is the critical discharge needed to move the D_{84}, as estimated from Ferguson (1994). Q_s (m^3/km^2/yr) is the bedload sediment transport capacity normalized to the drainage area A. $\dot{Q}_t$ (m/yr) is the total sediment transport capacity, derived from Q_s. Details of the calculation can be found in the paper.

4. Results and discussion

As mentioned earlier, Figure 4 shows the plot of cumulative probability distribution $P(\geq Q)$ against discharge Q. The vertical dashed lines represent the critical discharges needed to entrain bed material $Q_{c\ (D84)}$ for all three sites, as calculated earlier in Table 1. Discharge values greater than the critical discharge will start to entrain bed material. In other words, bedload starts to move when discharge values are to the right of the vertical line.

From Figure 4, we observe that for study site 11 on the River Maggia, daily mean discharges are expected to exceed critical discharge and move bed material about 26 days in a year. For study site 32 on the River Brenno, daily mean discharges are expected to exceed critical discharge about 220 days a year. Finally, for the most extreme case, daily mean discharges on study site 28 on the River Ticino are expected to exceed critical discharge all 365 days in year – in other words, the bedload is perpetually moving. Field observations, however, do not support that this estimation. A possible explanation for this incongruous prediction is that we have underestimated the critical discharge needed to move bedload. When we were measuring grain sizes in the field during data collection, we took care to measure only grains that had been obviously transported through fluvial processes, and avoided some of the larger grains that might have been locally introduced through mass-wasting processes, or were moraine deposits. Furthermore, Lenzi et al. (2006) point out that the larger grains in a channel increase the bed roughness and therefore increase flow resistance. Therefore, some fraction of shear stress would have been expended to overcome additional bedform resistance. The effective critical shear stress needed for entrainment would be greater than its theoretical value.

Results from analyzing the frequency-magnitude distribution of discharges in conjunction with the bedload transport capacity equation (Equation 7) are shown in Table 2.

Study Site	Total sediment transport capacity $\dot{Q}_t$ (m/yr)	Recurrence interval of most geomorphically-effective flood (days)
11	0.0263	86
28	0.167	1
32	0.0916	36

Table 2 shows the analysis of the frequency-magnitude distribution of discharges in conjunction with the bedload transport capacity equation.

The recurrence intervals of the most geomorphically-effective flood range from 1 day for site 32 to 86 days for site 11. While the result from site 28 is improbable for reasons discussed above, the key conclusion from Table 4 is that the maximum recurrence interval of the most geomorphically-effective flood (the flood that carries the most sediment) is at most 86 days or ~3 months. This is significant because, as mentioned in the 'Introduction', the most geomorphically-effective flood for alluvial rivers have a recurrence interval of one to two years, which at least several times greater than recurrence interval estimates in Table 4.

We conclude that frequent floods are more geomorphically-effective than rare, large floods in this region. Therefore, long-term erosion in the Lepontine Dome appears to be driven by very-frequent floods, which is in contrast to erosion patterns in arid climates where long-term erosion is driven by rare large floods (Jansen, 2006).

Table 2 also shows the total sediment transport capacity $\dot{Q}_t$ for all three sites ranging from 0.027 to 0.17 m/yr. On the other hand, erosion rates from the region have values of 0.00055 m/yr from long-term thermochronology (Devin McPhillips, personal communication) and 0.00027 m/yr from 10-Be dating (Wittman et al., 2008).

It is obvious that the total sediment transport capacity $\dot{Q}_t$ and erosion rates estimates differ by two to three orders of magnitudes. Furthermore, as Table 1 will show, the estimates of $\dot{Q}_t$ for all the 36 study sites (calculated using Equation 7 to 11) are also several orders of magnitude larger than the erosion rates of the region. There are several explanations for this large

difference. First, we have underestimated critical discharge values by at least an order of magnitude. Second, the power-law fit to the daily mean discharges was not suitable fit, either because daily mean discharges do not follow a power-law fit at very large discharges, or that we only have a relatively short time interval of discharge records (15 years) and hence the data is skewed by the small sample size. Third, the system is supply-limited, which means that the rivers are under-capacity.

We prefer the third explanation: Rivers in the Lepontine Dome are supply-limited and therefore not transporting as much sediment as they are capable of carrying. Consider that for transport-limited gravel bed rivers, channels self-form to maintain a dimensionless boundary shear stress τ^* equal to τ^*_c, where τ^* and τ^*_c have been measured to lie in the range 0.047–0.06 (Dede and Friend, 1998). However, for channels that are not transport-limited, dimensionless boundary shear stress τ^* values do not necessarily have to fall into this range.

Figure 5 is a plot of dimensionless boundary shear stress τ^* values against channel slope S. These values were calculated using Equation 8 and 11, using the variables channel slope S, width W and D_{84}, as well as the width-to-depth constant from Finnegan et al. (2005). The dark circles represent τ^* values calculated using D_{84} as the reference grain size of the bed material, while the light circles are τ^* values calculated using D_{50}. ($\tau^*_{(D50)}$ was also plotted to show that there is not a large difference in using either D_{50} or D_{84}.) The horizontal thick grey line represents $\tau^* = 0.06$, the expected value if these rivers were transport-limited alluvial channels.

Upon visual inspection, we note that all boundary shear stress τ^* values are far greater than the 0.06 value of transport-limited channels. None of the dark circles lie lower than the horizontal line in Figure 5. Instead τ^* varies between 0.09 to 3.3, two to five times greater than typical values for alluvial rivers. Dade and Friend (1998) mention that other than supply-limited

mountain rivers, such large values of critical shear stress have only been found in the entrainment of clay- to silt-sized particles in alluvial rivers. Whittaker et al. (2007) also found large values of τ^* from supply-limited mountain rivers in the Central Apennines, Italy, an area of active tectonic uplift.

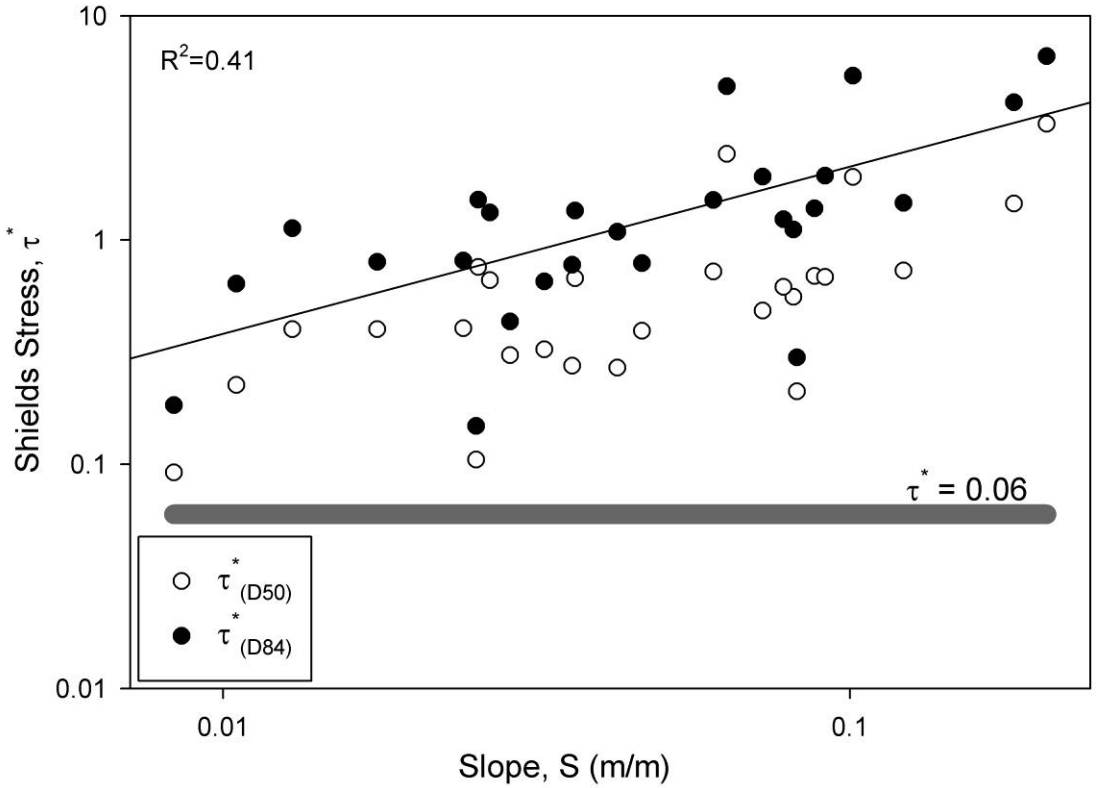

Figure 5 is a plot of dimensionless boundary shear stress τ^* against slope S. Dark circles represent τ^* calculated using D_{84} as the reference grain size; light circles are τ^* values calculated with D_{50}. $\tau^*_{(D84)}$ correlates moderately well with slope, with $r^2 = 0.41$. The horizontal solid grey line represents the Shields stress value for alluvial, transport-limited, self-forming gravel-bed rivers. This value is a constant and does not increase with slope. Note that all τ^* values (both dark and light circles) lie above this horizontal line, as these values are several times greater than the constant $\tau^* = 0.06$.

Furthermore, from Figure 5, shear stresses τ^* show a moderate correlation with slope ($r^2 = 0.41$). In alluvial rivers, shear stress values do not change with slope because channels respond to steepening by increasing grain size to maintain a constant critical shear stress of 0.047–0.06

(Whittaker et al., 2007). Grain sizes are the primary control of slopes. However, for the supply-limited rivers in the Lepontine Dome, this is not the case because there is a finite physical upper limit to the quantity and size of grains. Weathering controls the largest sizes of grains that can exist.

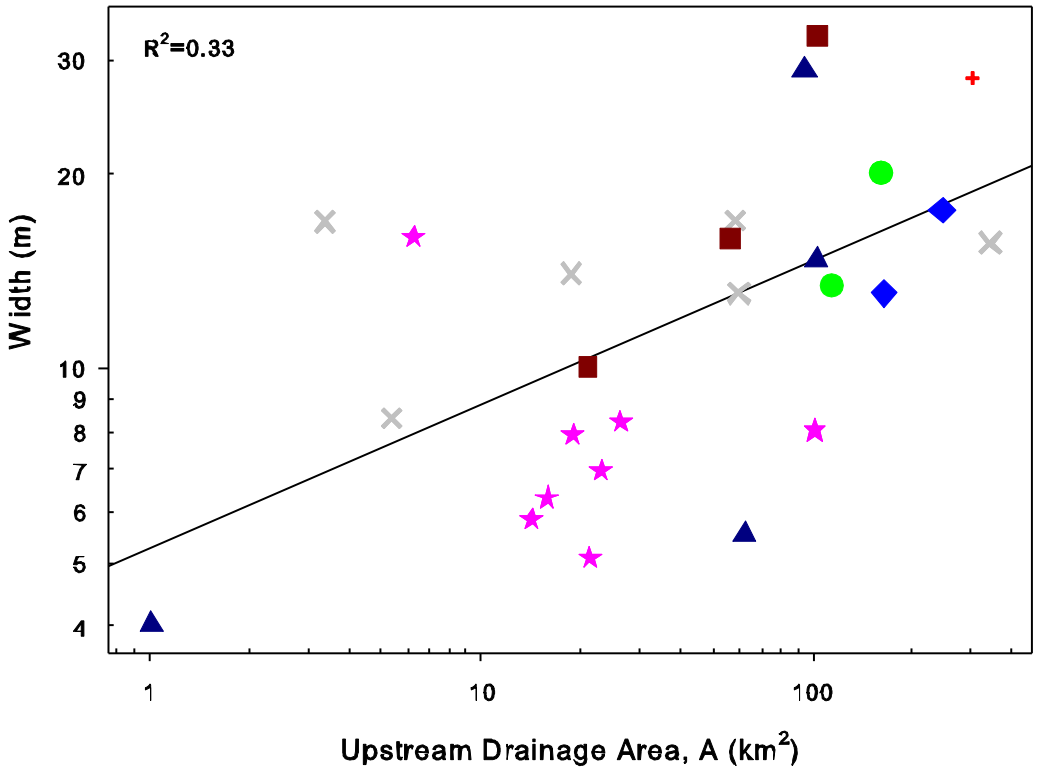

Figure 6 is a plot of bankfull width W_{bf} against upstream drainage area *A*. Similar symbols represent channel width measurements that were taken on the same rivers at different points along the stream. Note that the weak power-law fit for the both graphs (r^2= 0.33). Even channel width measurements taken along the same river do not show a strong correlation with drainage area, as evidenced by the scatter of similar symbols.

Figure 6 shows a plot of channel width *W* against upstream drainage area *A*, which shows a moderately-poor power-law fit to the points, where $W \sim A^{-0.22}$ and $r^2 = 0.33$. This moderately-poor fit is not typical of bedrock rivers that are in a topographic steady-state condition, which show a strong power-law relation where $W \sim A^{-b}$ and *b* ranges from 0.3 to 0.5 (Whittaker et al.,

2007). Furthermore, channel width taken at different points on the same river (similar symbols) show a wide scatter. The lack of correlation between channel width and drainage area, together with the supply-limited condition of the rivers, indicate that the rivers in the Lepontine Dome are undergoing a transient response to tectonics, in which tectonic uplift does not equal erosion rate.

5. Conclusions and direction for further research

The most geomorphically-effective flood for rivers in the Lepontine Dome are not the rare large events, but rather, very-frequent flood events that have recurrence intervals of less than a year. These frequent flood events are responsible for carrying the greater fraction of the annual sediment yield. This is because the estimated critical discharge or shear stress needed to move the bed material is so low that frequent lower-magnitude flood events are able to transport bedload.

There is good evidence that the rivers are supply-limited and under-capacity, as evidenced by the total sediment transport capacity $\dot{Q}_t$ of these rivers that is several orders of magnitude greater than the erosion rates of the region. This would imply that the rivers are undergoing a transient response to tectonic uplift and are not in equilibrium. What remains unknown is the reason why very-frequent flood events, with recurrence intervals of less than a year, are the most geomorphically-effective flood events, and how this frequency is related to the supply-limited condition of the rivers, if at all. In addition, the Lepontine Dome is an area that is known to have high erosion rates and intense precipitation, so the existence of rivers that are severely supply-limited and under-capacity to several orders of magnitude remains puzzling.

Further research should compare sediment transport and tectonic uplift between the anomalously-wet Lepontine Dome with the neighbouring dry Venosta Valley, whose rivers,

from preliminary field observations, appear to be transport-limited due to the prevalence of sediment deposits in the area.

6. Acknowledgements

This research was supported by a grant from the Keck Geology Consortium, which in turn was supported by the National Science Foundation.

7. References

Anders, A. M., D. Montgomery, et al. (2002). "Comparing Spatial Variations in Precipitation and Erosion Index to Differences in Long Term Exhumation Along the European Alps." 2002 Denver Annual Meeting.

Baker, V. R. and D. F. Ritter (1975). "Competence of rivers to transport coarse bedload material." Bulletin of the Geological Society of America 86(7): 975-978.

Costa, J. E. (1983). "Paleohydraulic reconstruction of flash-flood peaks from boulder deposits in the Colorado Front Range." Bulletin of the Geological Society of America 94(8): 986-1004.

Dede, W. B. and P. F. Friend (1998). "Grain-Size, Sediment-Transport Regime, and Channel Slope in Alluvial Rivers." The Journal of Geology 106(6): 661-676.

Ferguson, R. I. (1994). "Critical discharge for entrainment of poorly sorted gravel." Earth Surface Processes and Landforms 19(2): 179-186.

Finnegan, N. J., G. Roe, et al. (2005). "Controls on the channel width of rivers: Implications for modeling fluvial incision of bedrock." Geology 33(3): 229-232.

Frei, C. and C. Schär (1998). "A precipitation climatology of the Alps from high-resolution rain-gauge observations Int." J. Climatol 18: 873-900.

Howard, A. D. and G. Kerby (1983). "Channel changes in badlands." Bulletin of the Geological Society of America 94(6): 739-752.

Jansen, J. D. (2006). "Flood magnitude–frequency and lithologic control on bedrock river incision in post-orogenic terrain." Geomorphology 82(1-2): 39-57.

Komar, P. D. (1987). "Selective gravel entrainment and the empirical evaluation of flow competence." Sedimentology 34(6): 1165-1176.

Lenzi, M. A., V. D'Agostino, et al. (1999). "Bedload transport in the instrumented catchment of the Rio Cordon Part I: Analysis of bedload records, conditions and threshold of bedload entrainment." Catena 36(3): 171-190.

Lenzi, M. A., L. Mao, et al. (2006). "When does bedload transport begin in steep boulder-bed streams?" Hydrological Processes 20(16): 3517-3533.

Malamud, B. D. and D. L. Turcotte (2006). "The applicability of power-law frequency statistics to floods." Journal of Hydrology 322(1-4): 168-180.

Mueller, E. R. and J. Pitlick (2005). "Morphologically based model of bed load transport capacity in a headwater stream." J. Geophys. Res 110.

Werner, M. E. (2008). "Quantifying Rates of Erosion Using the Occurence and Magnitude of Flood Events in the Lepontine Dome, Switzerland." 2008 Northeastern Annual Meeting.
Whipple, K. X. (2004). "Bedrock rivers and the geomorphology of active orogens." Annual Review of Earth and Planetary Sciences 32(1): 151-185.
Whittaker, A. C., P. A. Cowie, et al. (2007). "Bedrock channel adjustment to tectonic forcing: Implications for predicting river incision rates." Geology 35(2): 103-106.
Williams, G. P. (1983). "Paleohydrological methods and some examples from Swedish fluvial environments. I. Cobble and boulder deposits." Geografiska Annaler 65(3-4).
Wittmann, H., F. von Blanckenburg, et al. (2007). "Relation between rock uplift and denudation from cosmogenic nuclides in river sediment in the Central Alps of Switzerland (DOI 10.1029/2006JF000729)." JOURNAL OF GEOPHYSICAL RESEARCH-ALL SERIES-112(F4): 4010.
Wohl, E. E. (2000). Mountain rivers, American Geophysical Union, Washington, DC.
Wolman, M. G. and J. P. Miller (1960). "Magnitude and frequency of forces in geomorphic processes: Jour." Geology 68: 54-74.